

SPIO : Gd-DTPA

1

2

3

4

: SPIO T2- (TSE), SPIO T2*- FISP
Gd-DTPA(, 가) (Fast low-angle shot, FLASH)

: 가 가 SPIO
25 , 36-70 (53.6) 20 , 가 5
. 가 가

SPIO receiver operating characteri-
stics(ROC)

: SPIO FISP SPIO T2- TSE
(p<0.05).
SPIO FISP 가 , SPIO T2- TSE,
(p<0.05). T2- TSE SPIO ,
FISP (p<0.05). ROC SPIO
T2- TSE FISP 가
(p<0.05).

: SPIO 가

가 raphy; CTAP) SPIO 가 (16, 17).

CT)

agent)

SPIO(superparamagnetic iron oxide)

Kupffer (reticuloen-
dothelial system)

가 가 (9-11). T2- SPIO 25 , 36-70 (53.6)
가 가 가 20 , 가 5 .

(12-15), CT (portog-

1

2

3

4

1999 9 1

1999 11 16

0.8 - 4.2cm (, 2.9cm) .)/ paired

1.5T (Mag-

netom Vision; Siemens, Erlangen, Germany)

(phased array multi-coil)

T2- (T2-weighted turbo spin echo,

T2-weighted TSE)(TR/TE/echo train lengths = 2,100/90/5,

2 , 192 × 256), T2*-

(Fast Imaging with Steady-State Precession,

FISP)(TR/TE = 180/12, 30 °, 1 , 120

× 256, 14 7) T1-

(Fast low-angle shot, FLASH)

(TR/TE = 135/4, 80 °, 120 × 256, 1)

MR , 가

, 24 SPIO

가 Gd-DT-

PA(Magnevist; Schering, Erlangen, Germany, 가

) 0.1mmol/kg 3-4ml/sec

, 10ml

, 30, 60, 180, 240

30 가

SPIO 100ml 5% 10

μmol/kg SPIO(Feridex; Advanced Magnetics,

Cambridge, U.S.A.) 30

10 2ml

4ml

. 2 SPIO

SPIO , , (re-

gion of interest, ROI) 가 가 ROI

ROI

(phase encoding direction)

. SPIO

(percentage of signal intensity

loss) : Percentage

of signal intensity loss = [(

) /] × (-100).

(contrast to noise ratio)

: = (-

student t-test . P 0.05

가

가 가(unac-

ceptable, 1), (poor, 2), (fair, 3), (good, 4)

(excellent, 5) 5 가

가 Wilcoxon signed

ranks test . P 0.05

가

Receiver operating characteristic(ROC)

ROC 2

, . ROC

37 , 56

, 465

ROC . ROC

2

465 MR

5

: 1 = (definitely or almost

definitely absent), 2 = (probably ab-

sent), 3 = (possibly present), 4 =

가 (probably present), 5 =

(definitely or almost definitely present).

MedCalc (MedCalc, Mariakerke, Belgium)

ROC 3

Table 1. Value for the Percentage of Signal Loss and the Liver-to-Lesion Contrast-to-Noise Ratio

	T2-TSE	FISP	Dynamic MR
PSIL			
Liver	41.62 ± 17.71	66.55 ± 15.15*	
CNR			
Unenhanced	3.71 ± 2.25	2.16 ± 6.26	
Enhanced	5.38 ± 4.12	13.20 ± 6.84 ⁺	10.18 ± 22.58

Note. - Data are given as mean ± standard deviation.

PSIL : percentage of signal intensity loss

= [(SI enhanced - SI unenhanced) / SI unenhanced] × 100

CNR : lesion-to-liver contrast-to-noise ratio

*, +: significant difference with T2-weighted TSE imaging (p< .05)

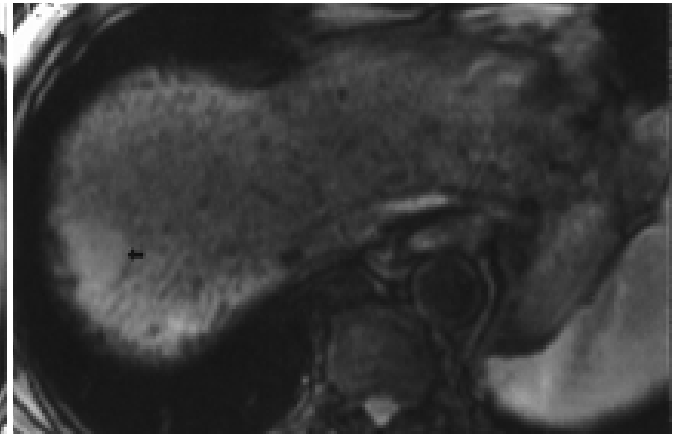
ROC ROC (Az) P ROC T2- TSE (p<0.05) (Fig. 1). SPIO FISP 가 (p>0.05).

Table 2

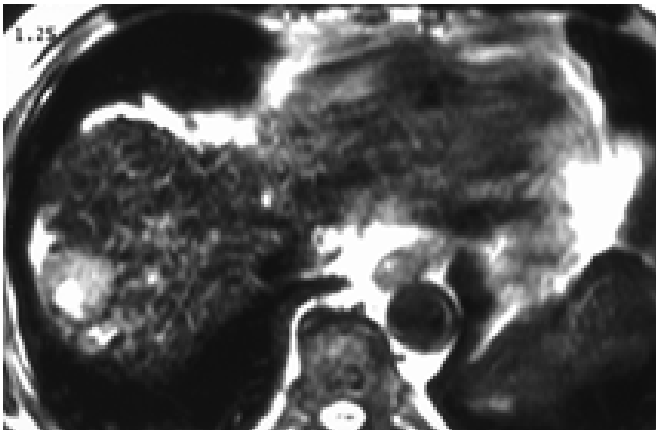
SPIO Table 1 SPIO FISP SPIO T2- FISP TSE, 가



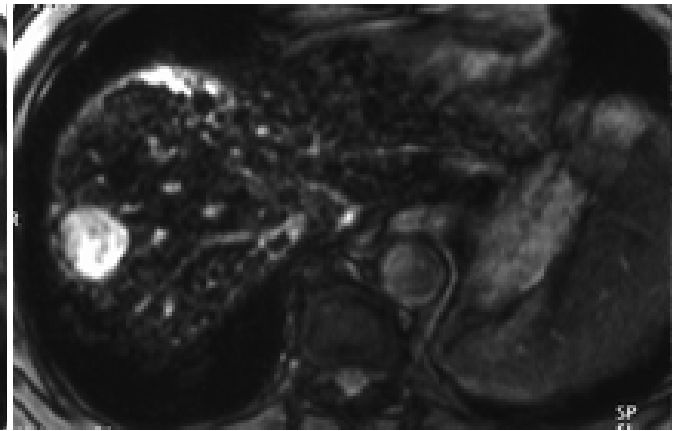
A



B



C



D



E

Fig. 1. 70-year-old man with a hepatocellular carcinoma in segment 8

A, B. SPIO-unenhanced T2-weighted TSE(A) and FISP images(B) show a HCC (arrow)with higher signal intensity than that of the normal hepatic parenchyma. Motion-related imaging artifacts obscure the left lobe of the liver.

C. On SPIO-enhanced T2-weighted TSE image, the tumor appears as to be hyperintense because of signal intensity loss of the normal liver parenchyma.

D. SPIO-enhanced FISP image shows higher liver-lesion contrast and high conspicuity than C due to homogeneous signal intensity loss of the normal liver parenchyma.

E. Early phase of dynamic gadolinium-enhanced imaging shows that the mass lesion displays rapid enhancement(arrow).

가 , SPIO T2- TSE, SPIO FISP
, SPIO
(p<0.05) (Fig. 2).
T2- TSE SPIO , FISP

(p<0.05).
ROC
ROC 465
ROC Table 3

Table 2. Results of Qualitative Analysis of Lesion Conspicuity and Imaging Artifact

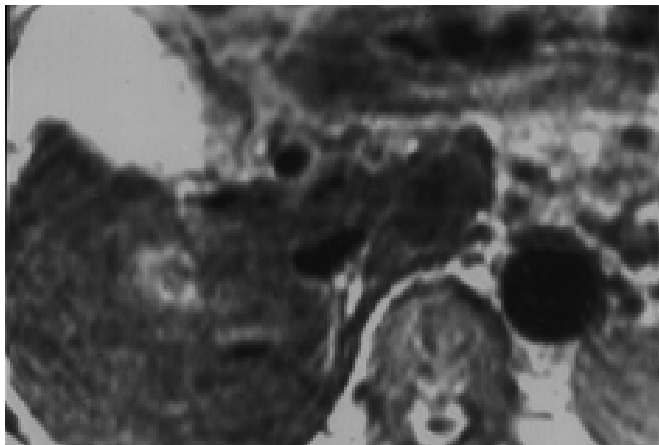
	Lesion Conspicuity	Imaging Artifact
T2-weighted TSE		
SPIO-unenhanced	3.2 ± 1.0	3.1 ± 0.8
SPIO-enhanced	4.2 ± 0.8*	3.3 ± 0.8
FISP		
SPIO-unenhanced	2.8 ± 1.2	4.1 ± 0.7**
SPIO-enhanced	4.5 ± 0.9*	4.5 ± 0.5**
Dynamic MR imaging	3.9 ± 0.9*	4.7 ± 0.5**

Note. - Data are given as mean ± standard deviation
* - significant difference with SPIO-unenhanced imaging (p< .05)
** - significant difference with T2-weighted TSE imaging (p< .05)

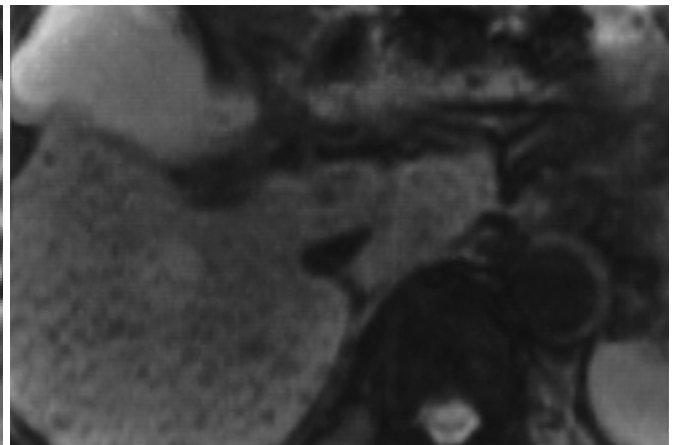
Table 3. Individual Az for Each Mortality

Imaging Technique	Az index		Mean Az
	Observer 1	Observer 2	
Dynamic MR imaging	0.896	0.944	0.913
Unenhanced MR imaging			
T2-TSE	0.860	0.935	0.894
FISP	0.757	0.832	0.790
SPIO-Enhanced MR imaging			
T2-TSE	0.941	0.995	0.966*
FISP	0.955	0.966	0.960*

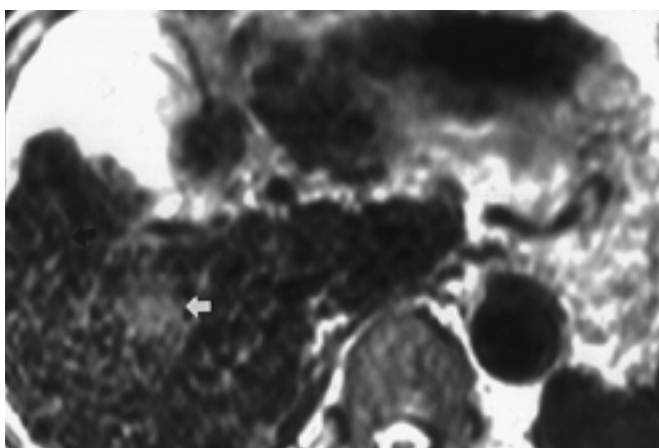
* - significant difference with dynamic MR imaging and SPIO-un-enhanced MR imaging
Az - area of binomial ROC curve.



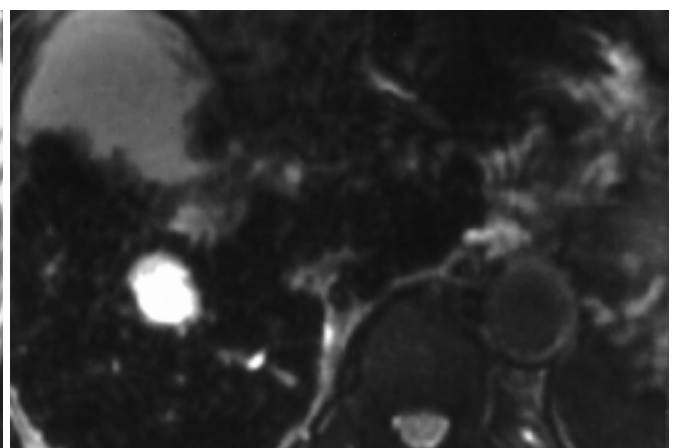
A



B



C



D

Fig. 2. 56-year-old man with severe liver cirrhosis and typical hepatocellular carcinoma.

A, B. SPIO-unenhanced T2-weighted TSE(A) and FISP image(B) show poor liver-lesion contrast.

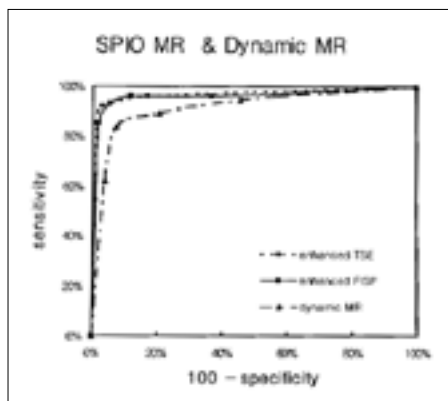
C. SPIO-enhanced T2-weighted TSE image shows poor conspicuity for demonstrating hepatic mass (white arrow) because of the presence of prominent fibrous septa (black arrow).

D. SPIO-enhanced FISP image shows excellent mass conspicuity than C.

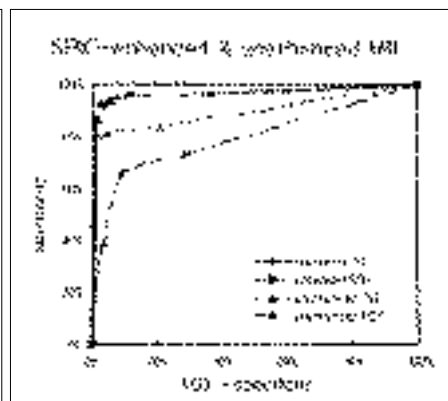
ROC 가 SPIO 가 (1-8),
T2- TSE FISP 가
(p<0.05) (Fig. 3), MR SPIO 가
SPIO FISP FISP T2- TSE FISP Kupffer (reticuloendothelial 가
(p<0.05). (Fig. 4). system) 가 (9-11). Kupffer 가
SPIO T2- TSE가 , S- MR T2- SPIO
PIO FISP 가 (Table 4). T2- SPIO MR 가
(12-15). SPIO
가 가 SPIO
가 가 (10, 19, 20), CTAP
(21). Yamamoto (22) S-
PIO 가 가
SPIO (18).

Table 4. Differentiation of Lesion Detection between SPIO-enhanced MR Imaging and Dynamic MR Imaging

Imaging Technique	Observer 1	Observer 2	Mean
Dynamic MR imaging			
Sensitivity	89.2	89.2	89.2
Specificity	67.9	91.1	79.5
Unenhanced MR imaging			
T2-TSE			
Sensitivity	75.7	86.5	81.1
Specificity	94.6	96.4	95.5
FISP			
Sensitivity	56.8	73.0	64.9
Specificity	92.9	89.3	91.1
SPIO-Enhanced MR imaging			
T2-TSE			
Sensitivity	86.5	97.3	91.9
Specificity	96.4	98.2	97.3
FISP			
Sensitivity	94.6	97.3	95.9
Specificity	83.9	92.9	88.4



3



4

Fig. 3. Composite receiver operating characteristic(ROC) curves. ROC curves show observer's confidence in detection of hepatocellular carcinomas on images obtained with dynamic gadolinium-enhanced FLASH, SPIO-enhanced FISP and TSE. Note higher sensitivity in SPIO-enhanced imaging than dynamic gadolinium-enhanced FLASH imaging ($p < .05$).

Fig. 4. Composite receiver operating characteristic(ROC) curves. ROC curves show observer's confidence in detection of hepatocellular carcinomas in images obtained with SPIO-unenhanced imaging than SPIO-unenhanced imaging ($p < .05$).

ced and SPIO- enhanced FISP and TSE imaging for the whole study. Note that observers were most sensitive in SPIO-enhanced imaging than SPIO-unenhanced imaging ($p < .05$).

T2- TSE 가 CT -FP , CTAP , SPIO ROC TSE 가 (segmental analysis) TSE T2- TSE가 가 FISP 가 T1- FLASH SPIO FISP SPIO ROC 가 SPIO T2- TSE SPIO T2- TSE FISP 가 SPIO T2- TSE SPIO FISP 가 Tang (18) 가 T1- SPIO T2*- FISP T2- TSE가 SPIO SPIO 가 SPIO T2- TSE가 SPIO FISP SPIO Tang (18) 가 가 SPIO Kupffer ROC 18 37

1. Semelka RC, Shoenut JP, Kroeker MA, et al. Focal liver disease: comparison of dynamic contrast-enhanced CT and T2-weight fat suppressed, FLASH and dynamic gadolinium enhanced MR imaging at 1.5T. *Radiology* 1992;184:687-694
2. Yamashita Y, Hatanaka T, Yamamoto H, et al. Differential diagnosis of focal liver lesions: role of spin-echo and contrast-enhanced dynamic MR imaging. *Radiology* 1994;193:59-65
3. Whitney WS, Herfkens RJ, Jeffrey RB, et al. Dynamic breath-hold multiplanar spoiled gradient-recalled MR imaging with gadolinium enhancement for differentiating hepatic hemangiomas from malignancies at 1.5T. *Radiology* 1993;189:863-870
4. Mitchell DG, Saini S, Weinreb J, et al. Hepatic metastasis and cavernous hemangiomas: distinction with standard- and triple-dose Gadoteridol-enhanced MR imaging. *Radiology* 1994;193:49-57
5. Yamashita Y, Fan ZM, Yamamoto H, et al. Spin-echo and dynamic gadolinium-enhanced FLASH MR imaging of hepatocellular carcinoma: correlation with histopathologic findings. *J Magn Reson Imaging* 1994; 4:83-90
6. Hamm B, Thoeni RF, Gould RG, et al. Focal liver lesions: characterization with nonenhanced and dynamic contrast material-enhanced MR imaging. *Radiology* 1994;190:417-423
7. Yoshida H, Itai Y, Ohtomo K, Kokubo T, Minami M, Yashiro N. Small hepatocellular carcinoma and cavernous hemangioma: differentiation with dynamic FLASH MR imaging with Gd-DTPA. *Radiology* 1989; 171:339-342
8. Yamashita, Mitsuzaki K, Yi T, et al. Small hepatocellular carcinoma in patients with chronic liver damage: prospective comparison of detection with dynamic MR and helical CT of the whole liver. *Radiology* 1996;200:79-84
9. Fetis CJ, Elizondo G, Weissleder R, et al. Superparamagnetic oxide-enhanced MR imaging: pulse sequence optimization for detection of liver cancer. *Radiology* 1989;172:393-397
10. Tsang YM, Stark DD, Chen MC, Weissleder R, Wittenberg J, Ferrucci JT. Hepatic micrometastasis in the rat: ferrite-enhanced MR imaging. *Radiology* 1988;167:21-24

11. Saini S, Stark DD, Hahn PF, et al. Ferrite particles: a superparamagnetic MR contrast agent for enhanced detection of liver carcinoma. *Radiology* 1987;162:217-222
12. Weissleder R. Liver MR imaging with iron oxides: toward consensus and clinical practice(editorial). *Radiology* 1993;193:593-595
13. Ros PR, Freeny PC, Harms SE, et al. Hepatic MR imaging with ferumoxides: a multicenter clinical trial of the safety and efficacy in the detection of focal hepatic lesions. *Radiology* 1995;196:481-488
14. Winter TC III, Freeny PC, Nghiem HC, et al. MR imaging with i.v. superparamagnetic iron oxide: efficacy in the detection of focal hepatic lesions. *AJR* 1993;161:1191-1198
15. Schwartz LH, Seltzer SE, Tempany CMC, et al. Superparamagnetic iron oxide hepatic MR imaging: efficacy and safety using conventional and fast spin-echo pulse sequences. *J Magn Reson Imaging* 1995;5:566-570
16. Seneterre E, Taourel P, Bouvier Y, et al. Detection of hepatic metastases: ferumoxides-enhanced MR imaging versus unenhanced MR imaging and CT during portography. *Radiology* 1996; 200:785-792
17. Soyer P. Will ferumoxides-enhanced MR imaging replace CT during arterial portography in the detection of hepatic metastases? prologue to a promising future. *Radiology* 1996;200:610-611
18. Tang Y, Yamashita Y, Arakawa A, et al. Detection of hepatocellular carcinoma arising in cirrhotic livers: comparison of gadolinium- and ferumoxides-enhanced MR imaging. *AJR* 1999;172:1547-1554
19. Fretz CJ, Stark DD, Metz CE, et al. Detection of hepatic metastasis: comparison of contrast-enhanced CT, unenhanced MR imaging, and iron-oxide-enhanced MR imaging. *AJR* 1990;155:763-770
20. Stark DD, Weissleder R, Elizondo G, et al. Superparamagnetic iron oxide: clinical application as a contrast agent for MR imaging of the liver. *Radiology* 1988;168:297-301
21. Seneterre E, Taourel P, Bouvier Y, et al. Detection of hepatic metastasis: ferumoxides-enhanced MR imaging versus unenhanced MR imaging and CT during arterial portography. *Radiology* 1996; 200:785-792
22. Yamamoto H, Yamashita Y, Yoshimatsu S, et al. Hepatocellular carcinoma in cirrhotic liver: detection with unenhanced and iron oxide-enhanced MR imaging. *Radiology* 1995;195:106-112

Detectability of Hepatocellular Carcinoma: Comparison of Gd-DTPA-Enhanced and SPIO-Enhanced MR Imaging¹

Hyo-Sung Kwak, M.D., Jeong-Min Lee, M.D., In-Hwan Kim, M.D.,
Chong-Soo Kim, M.D., Hyeun-Young Han, M.D.², Kwon-Ha Yoon, M.D.³, Kyung-Sook Shin, M.D.⁴

¹Department of Diagnostic Radiology, Chonbuk National University Medical School

²Department of Diagnostic Radiology, Eulgy University Medical School

³Department of Diagnostic Radiology, Wonkwang University Medical School

⁴Department of Diagnostic Radiology, Chungnam National University Medical School

Purpose : To compare the detectability of hepatocellular carcinoma (HCC) using superparamagnetic iron oxide (SPIO)-enhanced T2-weighted turbo spin echo (TSE), SPIO-enhanced T2*-weighted FISP, and dynamic Gd-DTPA-enhanced fast low-angle shot (FLASH) MR images.

Materials and Methods : In order to assess their hepatic lesions, 25 patients (20 men and 5 women) with HCC were enrolled in an MR study in which both gadolinium and SPIO were used. Since the lesions were most conspicuous during the phase of dynamic arterial dominant phase of dynamic gadolinium-enhanced imaging, this was the phase used for analysis. Images were analyzed qualitatively and quantitatively, and to compare the diagnostic value of gadolinium-enhanced imaging with that of SPIO-enhanced imaging for the detection of HCCs, a receiver-operated characteristic curve was obtained.

Results : Qualitative analysis revealed a significantly higher percentage of signal loss and a higher liver-lesion contrast-to-noise ratio on SPIO-enhanced FISP imaging than on SPIO-enhanced T2-weighted TSE imaging ($p < 0.05$). It also showed that the lesions were most clearly visible on SPIO-enhanced FISP imaging (and significantly so), followed by SPIO-enhanced T2-weighted TSE imaging, and dynamic gadolinium-enhanced imaging. Imaging artifacts were more prominent on SPIO-enhanced T2-weighted TSE than on SPIO-enhanced FISP imaging or dynamic gadolinium-enhanced imaging ($p < 0.05$). According to ROC analysis, SPIO-enhanced T2-weighted turbo spin echo (TSE) or SPIO-enhanced FISP imaging achieved higher accuracy than did dynamic gadolinium-enhanced FLASH imaging ($p < 0.05$).

Conclusion : For the detection of hepatocellular carcinomas, SPIO-enhanced MR imaging is better than gadolinium-enhanced FLASH imaging.

Index words : Liver, MR

Liver neoplasms, MR

Magnetic resonance (MR), contrast agents

Magnetic resonance (MR), comparative studies

Address reprint requests to : Jeong-Min Lee, M.D., Department of Diagnostic Radiology, Chonbuk National University Medical School
#634-18 Keumam-Dong, Chonju-shi, Chon Buk 561-712, Korea.
Tel. 82-652-250-1152 Fax. 82-652-272-0481